EARTHQUAKE ACTIVITY IN THE GREATER NEW YORK CITY AREA: A FAULTFINDER'S GUIDE

ALAN L. KAFKA
Weston Observatory
Department of Geology and Geophysics
Boston College
Weston, MA 02193

MARGARET A. WINSLOW
Department of Earth and Planetary Sciences
City College of CUNY
New York, NY 10031

NOEL L. BARSTOW
Rondout Associates, Inc.
Stone Ridge, NY 12484

INTRODUCTION: EARTHQUAKES IN THE NORTHEASTERN UNITED STATES

Although the area within a 100 km radius of New York City is clearly not as seismically active as most areas near plate boundaries, this area has had its share of moderate earthquake activity. For most earthquakes in the interior of the North American plate--unlike the situation along plate boundaries--it is not clear whether geologic faults mapped at the surface are the faults along which the earthquakes are occurring. The purpose of this field trip is to examine several geologic features in the greater New York City (NYC) area that might be related to earthquake activity. As we proceed, the following question will be addressed:

Are seismically active faults in the NYC area delineated by geological features that are observable at the earth's surface?

To understand earthquake phenomena in the NYC area, it is helpful to picture this area in the context of earthquake activity throughout the northeastern United States (NEUS). The NEUS has one of the longest records of reported earthquake activity in North America (Fig. 1). Earthquake activity was noticed in this region by early European settlers, and as the population density grew, an increasing number of earthquakes were reported. These earthquakes were usually minor, but sometimes not-so-minor, and occasionally even caused damage. Instrumental seismic monitoring in the NEUS began in the early 1900's, and routine reporting of instrumentally recorded earthquakes began in 1938 with the initiation of the Northeastern Seismic Association (Linehan and Leet, 1942). The first telemetered regional seismic network was operated in northern New England by Weston Observatory from 1962 to 1968, but it was not until the early 1970's that the present regional networks were established. The number of seismic stations in the NEUS steadily increased between 1970 and 1974. By 1975, a number of institutions operating seismic networks in the region formed a cooperative group known as the Northeastern United States Seismic Network (NEUSSN; Fig. 2). The data recorded by the NEUSSN has enhanced our ability to study the regional seismic activity. Analysis of these data provides insight into the possible causes of the earthquakes.

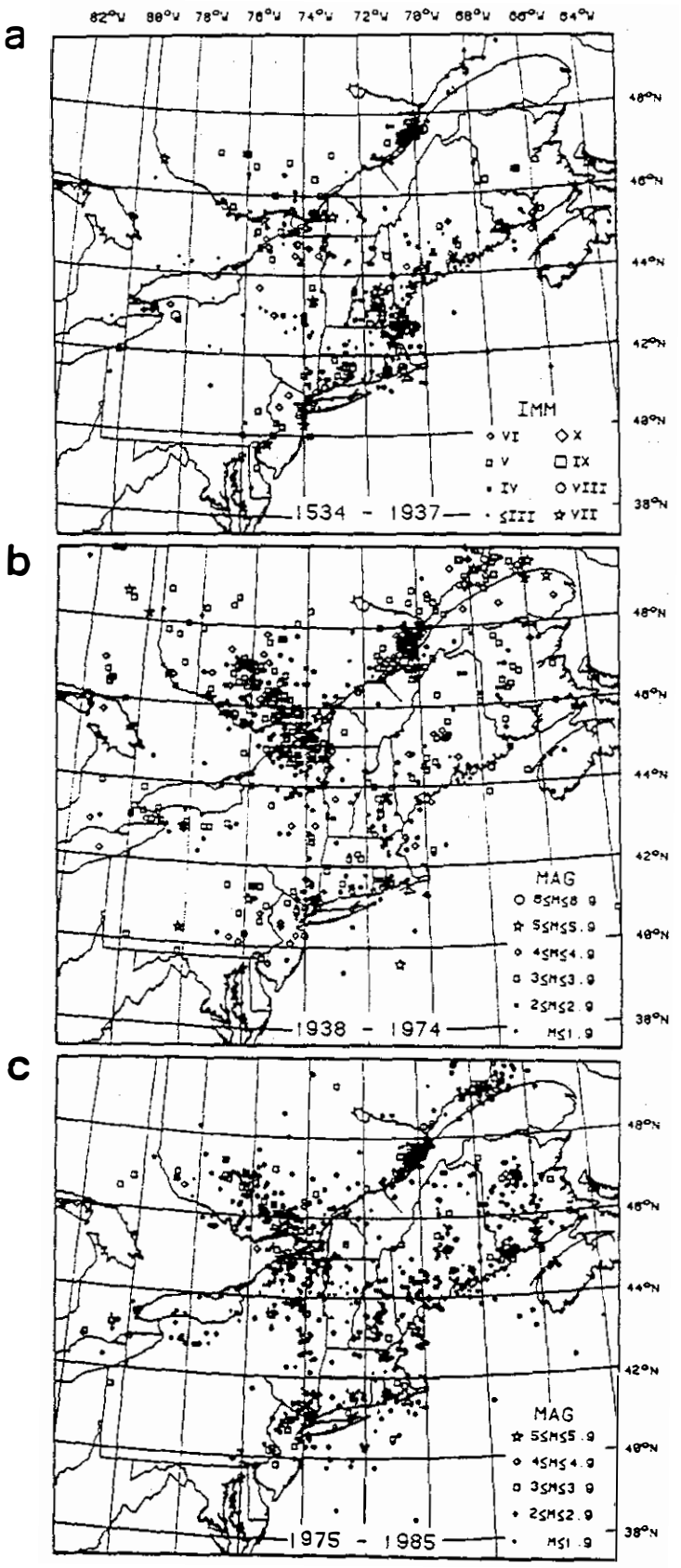

HISTORICAL

EARLY INSTRUMENTAL

NETWORK

Figure 1.

Seismicity in the northeastern United States and adjacent areas.

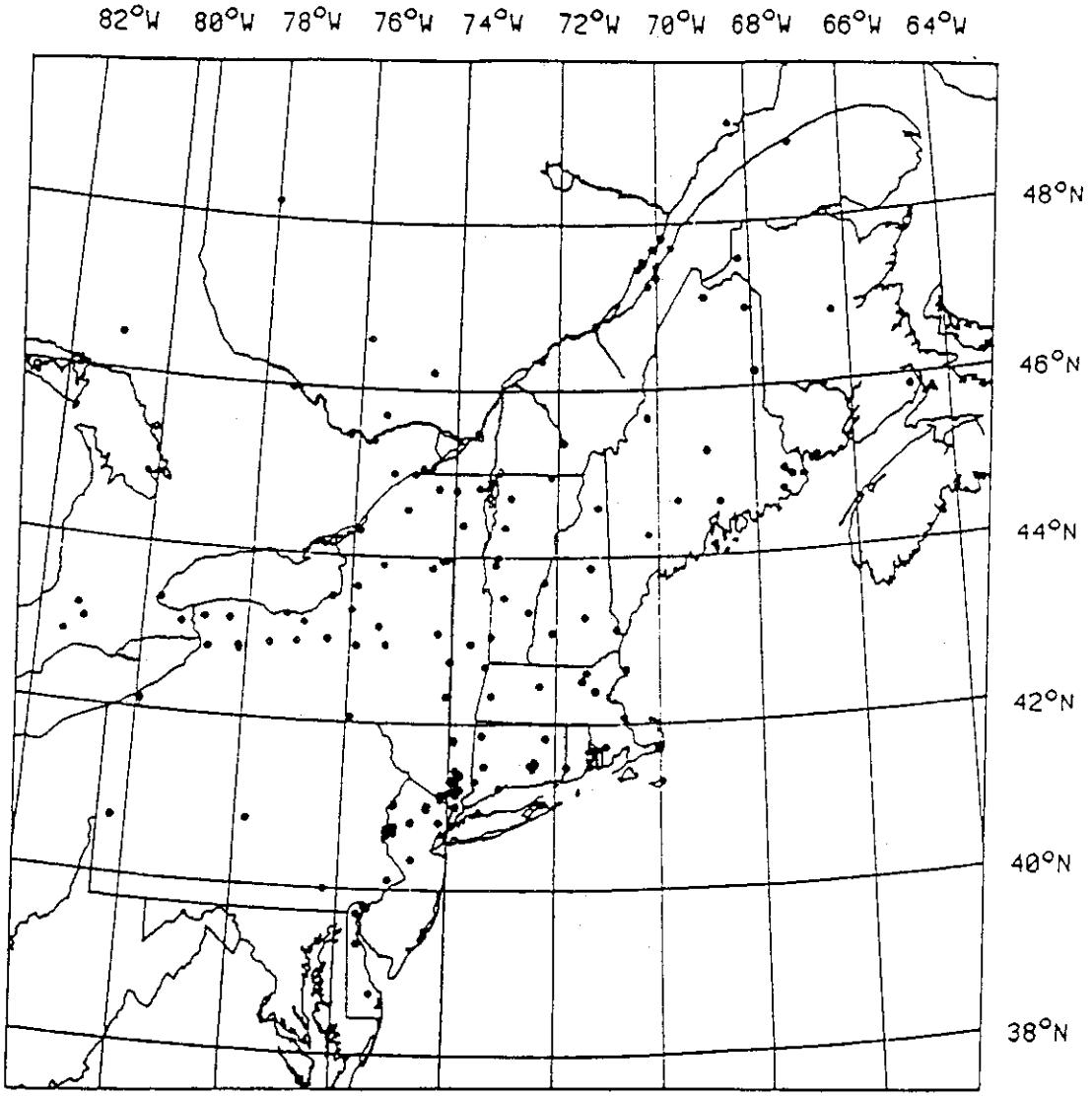

Figure 2. Stations of the Northeastern United States Seismic Network (NEUSSN). These stations are operated by Weston Observatory of Boston College, Lamont-Doherty Geological Observatory of Columbia University, Massachusetts Institute of Technology, Woodward-Clyde Consultants, State University of New York at Stony Brook, Pennsylvania State University, and Delaware Geological Survey.

Since at present the NEUS is not located on or near an active plate boundary, there is no obvious plate tectonic interpretation of why earthquakes occur here. The present-day tectonic setting of the region is a passive continental margin. The nearest plate boundaries are the mid-Atlantic ridge to the east, the subduction/transform system along the western margin of North America to the west, and the northern boundary of the Caribbean plate to the south. All of these plate boundaries are located several thousand kilometers from the NEUS. The last major tectonic activity in this region postdates the Triassic separation of North America from Africa and occurred in the latter part of the Mesozoic. This activity is delineated by igneous rocks found in the Connecticut and Newark Mesozoic basins, in the White Mountain magma series of New England, in the Montregian Hills of southern Quebec, and along the New England seamount chain. In the more distant geologic past, the area experienced at least two continental collision and rifting episodes, of which the Appalachian mountain system is a remnant expression (Bird and Dewey, 1970; Skehan, 1988; Skehan and Rast, 1983). While the present-day seismicity is quite low compared to that of most plate boundaries, its persistence and its potential for producing damaging earthquakes make it the subject of both scientific inquiry and public concern.

The following three fundamental, and as yet unanswered, questions provide the underlying framework for our analysis of NEUS earthquakes:

- What are the forces that cause earthquakes in this area?
- Which geologic or tectonic features are seismically active?
- What is the potential for future large earthquakes?

With these questions in mind, we will summarize the current understanding of earthquake phenomena in the NEUS, with particular emphasis on the NYC area.

THE PROBLEM WITH MAGNITUDES

Before we summarize the seismic activity in the NEUS, it is important to mention that there are some unresolved issues regarding magnitudes of earthquakes in the NEUS. Magnitudes reported in the Bulletins of the NEUSSN are reported as m_N, where "N" refers to the Nuttli (1973) m_{bLg} magnitude scale. The Nuttli magnitude formulas were developed for estimating body wave magnitude (m_b) from 1 Hz Lg waves (a superposition of Love waves and higher-mode Rayleigh waves), which are recorded from more distant earthquakes. However, the seismograms of small earthquakes (m_b < about 4.0) recorded at shorter distances by stations of the NEUSSN are generally dominated by higher-frequency (~5-10 Hz) Lg waves. It is the amplitudes of these higher-frequency waves that are used along with the Nuttli (1973) formulas to estimate magnitudes for reporting earthquakes in the NEUSSN bulletins. The relationship between these reported m_N magnitudes and m_b is not well known.

For earthquakes that are large enough that the recorded seismograms are clipped (i.e. off-scale), but not large enough to be recorded globally, magnitude formulas were developed that use signal duration (sometimes called "coda-length") instead of amplitude as an estimate of the size of the event. The m_C magnitude scale was developed for the NEUS from a study of the relationship between coda-length and m_N (Rosario, 1979; Chaplin et al., 1980). The purpose of using m_C is to provide an estimate

of m_N when amplitude measurements are not available, and m_C is reported as the magnitude for some of the events in the NEUSSN bulletins.

The magnitudes shown for events in Fig. 1(c) are those listed in the NEUSSN computer files, and most are listed as m_N or m_C. To compare the seismicity shown in Fig. 1(c) with that in other parts of the world, it is necessary to estimate the relationship between "m_N or m_C" and some more generally used magnitude scale. Fig. 3(a) shows the relationship between "m_N or m_C" (as reported in the NEUSSN Bulletins) and m_{bLg} for 19 events in the NEUS and adjacent Canada. The slope of the regression line in Fig. 3(a) is 1.14, and the average difference between "m_N or m_C" and m_{bLg} is 0.4 magnitude units (with "m_N or m_C" overestimating m_{bLg}). Thus, although the problem with NEUS magnitudes is not yet resolved, the magnitudes shown in Fig. 1(c) should be considered to be approximately correct in a relative sense, but they appear to overestimate m_b by about 0.4 magnitude units.

SPATIAL DISTRIBUTION OF EARTHQUAKE ACTIVITY IN THE NORTHEASTERN UNITED STATES

In the next three sections, we summarize the current understanding of earthquake activity in the NEUS to provide a framework for our discussion of earthquake activity in the NYC area. Locations of the older epicenters in Fig. 1(a) are based upon felt reports, while the locations of earthquakes since the 1930's have been determined primarily from instrumental data. The earthquakes shown in Fig. 1 indicate that much of the area is seismically active but that the distribution of earthquake activity is not spatially uniform. All of the zones that have been seismically active throughout the historical record (including the NYC area) are also seen to be active in the instrumental records. The largest earthquakes in the NEUS have all occurred in one or another of these active areas. There is a general correlation between the spatial distribution of epicenters determined from the network data and that of the historical seismicity. The general features of the pattern of seismicity have been fairly stable since about the mid-1500's. Thus, it appears that whatever the process is that causes earthquakes in this region, that process has been spatially stable for the past several hundred years.

The largest earthquakes recorded in the NEUS are: the 1727 and 1755 earthquakes located near Cape Ann, Massachusetts; the 1904 earthquake in eastern Maine; the 1929 earthquake in western New York; the 1940 earthquakes in central New Hampshire; the 1944 earthquake at the northern New York/Canadian border; the 1983 earthquake in north central New York, and (most relevant to this field trip) the 1884 earthquake near NYC. All of these earthquakes caused at least minor damage, and all of them (except perhaps the 1884 NYC event) probably exceeded m_b 5.0 (Street and Turcotte, 1977; Street and Lacroix, 1979). The largest earthquake known to have occurred in the NEUS is the 1755 Cape Ann earthquake. The maximum intensity for that event has been estimated to be VIII on the Modified Mercalli (MM) scale (Weston Geophysical, Inc., 1977). The Cape Ann earthquake caused damage in Massachusetts, New Hampshire and Maine and was felt as far away as Washington, DC. Street and Lacroix (1979) estimated the magnitude of the Cape Ann earthquake to be approximately m_b 6.0.

Rockwood (1885) investigated the 1884 NYC earthquake, and he reported fallen bricks and cracked plaster from eastern Pennsylvania to central Connecticut. The

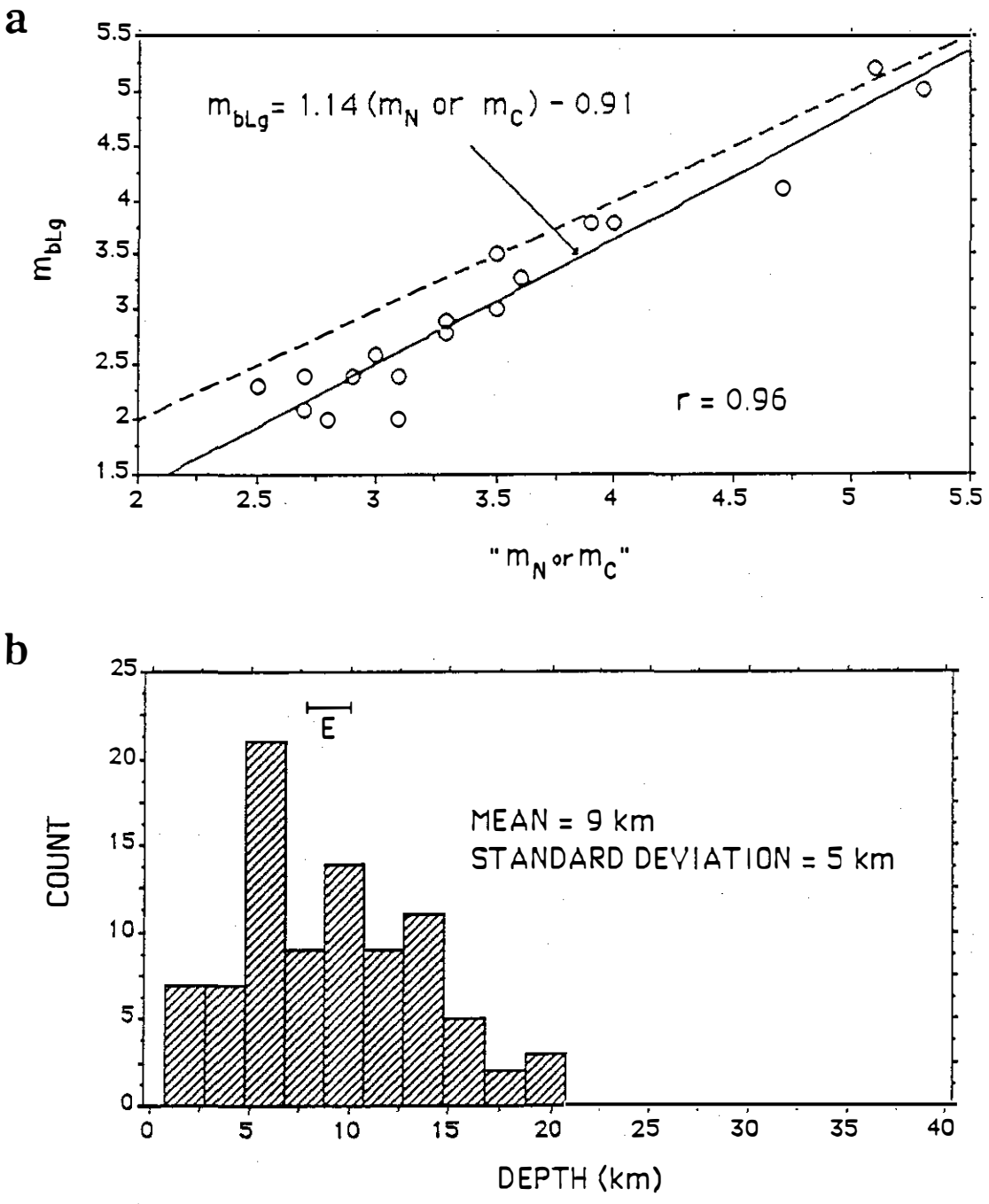

Figure 3. (a) Relationship between "m_N or m_C" and m_{bLg} (from Kafka, 1988). The value of "m_N or m_C" is the magnitude that was sorted from the NEUSSN data (as described in the text). The dashed line is the locus of points for which "m_N or m_C" equals m_{bLg}. (b) Histogram of depths of earthquakes recorded by the NEUSSN in the northeastern United States from1975 to 1983. Bar labelled E indicates the range of depths that Ebel et al. (1986) found from teleseismic waveform modelling of some of the largest earthquakes in North America.

maximum intensity reported by Rockwood was at two sites on western Long Island (Jamaica, New York and Amityville, NY). The felt area of the 1884 earthquake, measured from the map published by Rockwood, was about 270,000 km^2. Smith (1966) reported a maximum MM intensity of VII for the 1884 NYC earthquake, which suggests a magnitude on the order of m_b 5.0 for that event.

The occurrence of the 1755 Cape Ann earthquake and the 1884 NYC earthquake provides minimum values for the size of earthquakes that can be expected to occur in the NEUS in general (m_b of about 6.0) and in the NYC area in particular (m_b of about 5.0). In order to make more specific predictions of the maximum magnitude earthquakes that can occur at a particular location in the NEUS, it is necessary to know which faults (or other features) are active, as well as the record of seismic activity for those features. Unfortunately, however, there are few (if any) surface-mapped faults in the NEUS that have been confirmed to be active. Thus, at the present time, we must be satisfied with only general conclusions regarding where and when future large earthquakes will occur in the NEUS.

DEPTH OF EARTHQUAKE ACTIVITY

Although the relatively low density of regional seismic stations limits the resolution of focal depth for many of the events, the station density is sufficient to conclude that earthquakes in the area generally occur in the upper half of the crust. The deepest hypocenters located by the NEUSSN stations generally occur at about 20 km, and the shallowest earthquakes are about 1 km deep (Pomeroy et al., 1976; Ebel et al., 1982; Mrotek et al., 1988). Events deeper than 20 km tend to occur more frequently in adjacent Canada rather in the NEUS. Earthquakes as deep as 33 km have been reported in the Charlevoix seismic zone--a cluster of activity centered at about 47.5° N, 70.3° W (Fig. 1).

To summarize the depth distribution of earthquakes recorded in the NEUS, Ebel and Kafka (1989) analyzed the depths reported for a sample of earthquakes from the NEUSSN bulletins. This sample consisted of all events recorded between 1975 and 1983. From those events they extracted all earthquakes for which there was (a) at least one station located within a distance of twice the depth; and (b) a total of at least four stations recording the event. A histogram of those data is shown in Fig. 3(b). For that set of data, the mean depth is 9 km and the standard deviation is 5 km. Because of the requirement of at least one nearby station, the depths shown in the histogram are probably biased toward deeper events (which would be more likely to be recorded by a station within twice the depth). From Fig. 3(b) it appears that the earthquake activity tends to cluster in a zone between about 5 and 15 km beneath the earth's surface (although events shallower than 5 km could be more numerous than Fig. 3(b) implies since they were systematically excluded from these statistics).

An independent measure of the depth range where the larger earthquakes tend to occur in this region can be obtained from the results of waveform modelling of larger earthquakes that were recorded teleseismically. Also shown in Fig. 3(b) is the range of depths that Ebel et al. (1986) found from teleseismic waveform modelling of the largest earthquakes of this century in northeastern North America. Those events were found to occur at depths ranging from 8 to 10 km. In addition, Nabelek (1984) and Basham and Kind (1986) modelled teleseismic waveforms from the January 9, 1982 earthquake in New Brunswick, Canada (m_b=5.7). They concluded that the depth of that event was 6 km. Similar depth ranges were observed from aftershock

surveys of larger earthquakes. For example, Seeber et al. (1984) found that aftershocks of the 1983 Goodnow, NY earthquake (m_b=5.1) were confined to a depth range of 7 to 8.5 km.

All of these depth estimates suggest that NEUS earthquakes occur in the upper 20 km of the crust. This depth range for NEUS earthquakes is consistent with the idea that only the upper half of the crust behaves in a brittle fashion (Kirby, 1980).

STRESS FIELD AND MAPPED FAULTS

The most commonly accepted explanation for the cause of earthquakes in the NEUS is that ancient zones of weakness are being reactivated in the present-day stress field (Sykes, 1978). In this model, preexisting faults and zones of weakness from earlier orogenic episodes persist in the intraplate crust, and, by way of analogy with plate boundary seismicity, earthquakes occur when the present-day stress is released along these zones of weakness. Much of the recent research on the cause of NEUS earthquakes has, therefore, involved attempts to identify preexisting faults and determine whether they are favorably oriented so as to be reactivated by the present-day stress field. While this concept of reactivation of old zones of weakness is commonly assumed, the identification of individual active geologic features has proven to be quite difficult. It is not at all clear whether faults mapped at the earth's surface in the NEUS are the same faults along which the earthquakes are occurring.

State of Stress

The intraplate stress field in the NEUS is generally assumed to be the result of a combination of forces generated by plate tectonic processes. Two large-scale sources of stress that have been considered in a number of studies are asthenospheric drag and ridge push (Richardson et al., 1979). Another source of stress that could be significant in plate interiors is asthenospheric counterflow (Chase, 1979; Hager and O'Connell, 1979). Within the context of the ancient zones of weakness hypothesis, it is important to characterize accurately the observed modern stress field to determine whether preexisting faults are favorably oriented to be reactivated.

In an effort to summarize the present state of knowledge regarding the stress field in the NEUS, Ebel and Kafka (1989) reviewed data from focal mechanism studies in the NEUS and adjacent parts of Canada (Figs. 4 and 5). Focal mechanisms can be described by specifying the directions of the so-called *pressure axis* (or P-axis) located in the center of the dilatational quadrant and *tension axis* (or T-axis) located in the center of the compressional quadrant. Fig. 4 shows the azimuths of the horizontal component of P-axes from numerous studies superimposed on a map of the region. Fig. 5 shows equal area stereographic plots of the P-axes and the T-axes from the various studies analyzed by Ebel and Kafka (1989). The average P-axis and T-axis for this data set was determined by vectorially averaging all of the axes which intercept a given focal hemisphere. The P-axes tend to cluster toward the east and west directions. The average P-axis was found to have an azimuth of 266° and a plunge of 1°. The average T-axis was found to have an azimuth of 105° and a plunge of 88°.

These focal mechanism results are consistent with a regional stress field for the entire NEUS and adjacent Canada in which the maximum compressive stress is essentially horizontal and trends approximately east. The minimium stress, as

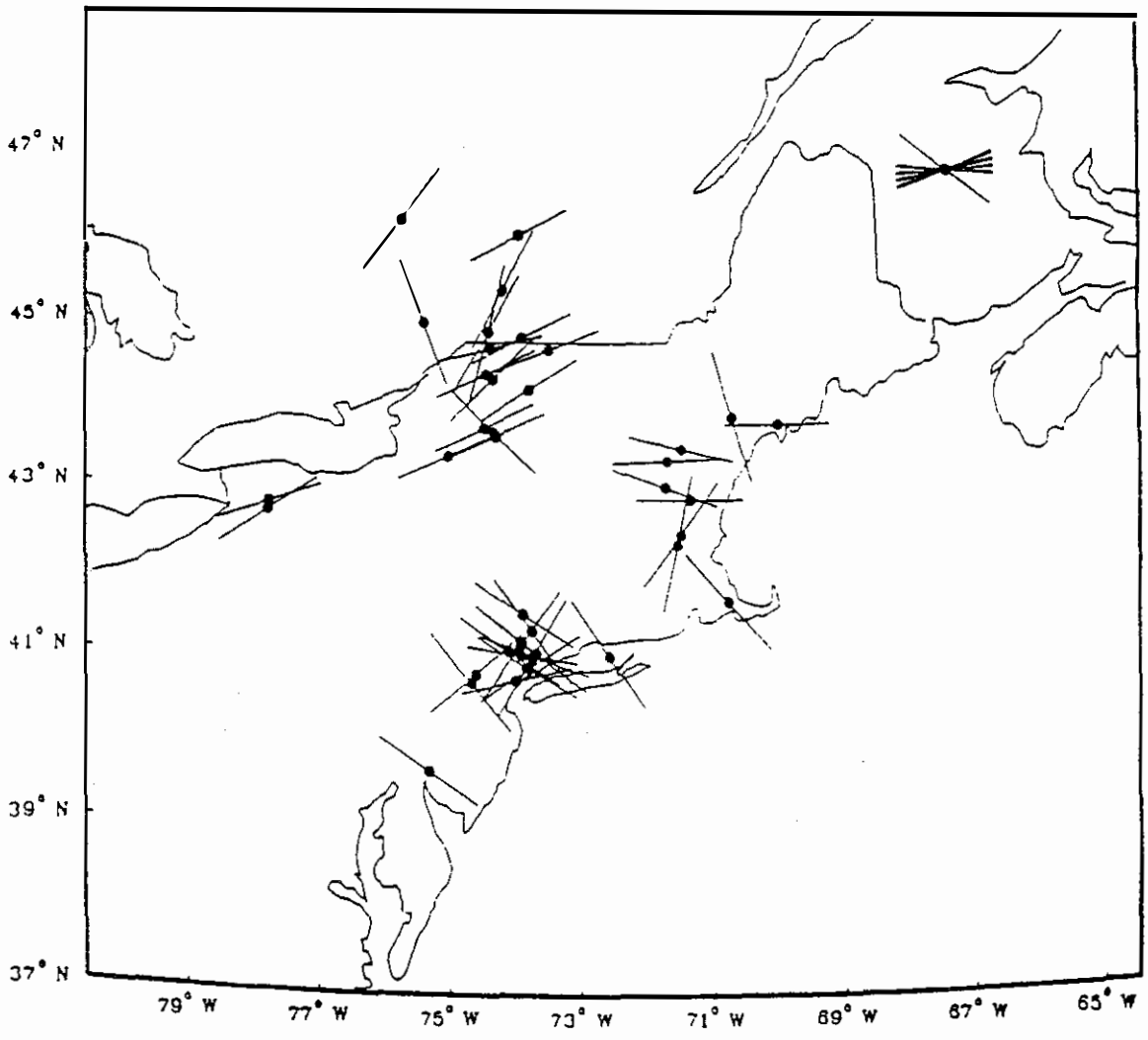

Figure 4. Map showing azimuths of P-axes from focal mechanisms of earthquakes in the northeastern United States. The data shown here were taken from references listed in caption of Figure 5.

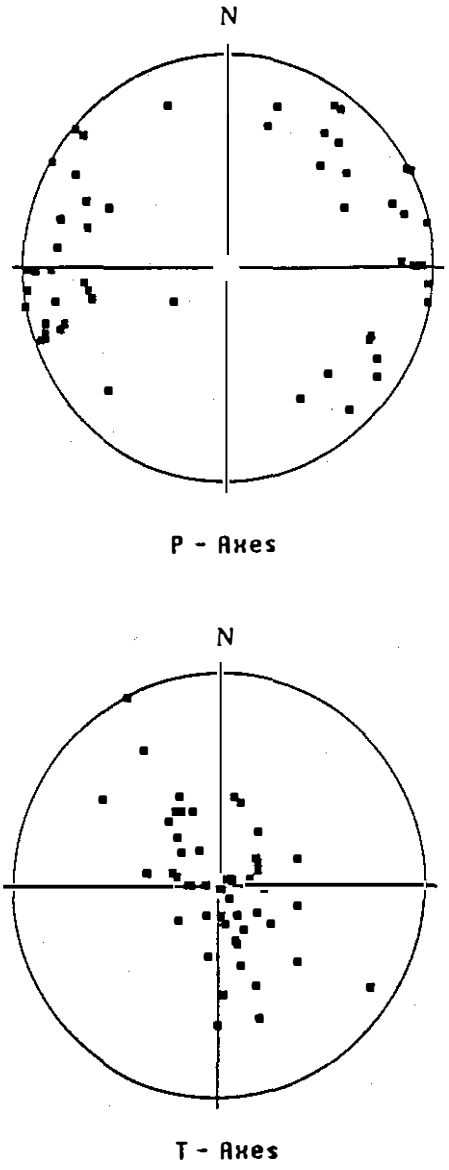

Figure 5. Lower hemisphere stereographic plots of P-axes and T-axes of earthquakes in the northeastern United States. The data shown here were taken from the following studies: Sbar et al. (1970, 1972, 1975), Herrmann (1979), Horner et al. (1978), Graham and Chiburis (1980), Yang and Aggarwal (1981), Pulli and Toksoz (1981), Kafka (1982), Kafka et al. (1982), Schlesinger-Miller et al. (1983), Wetmiller et al. (1984), Wahlstrom (1985), Quittmeyer et al. (1985), and Filipkowski (1986). The P-axes tend to cluster in the east and west directions, and the T-axes tend to cluster in the vertical direction. The average P-axis for this data set has an azimuth of 266° and a plunge of 1°. The average T-axis for this data set has an azimuth of 105° and a plunge of 88°.

inferred from the average T-axis, is nearly vertical. There is, however, no reason to assume that the stress field doesn't vary (temporally and/or spatially) across the region studied.

Seismicity and Mapped Faults

If the stress field in the upper crust can be accurately characterized, and if reactivation of ancient faults is the cause of NEUS earthquakes, then seismically active features could be delineated by identifying the faults and determining their orientation relative to the stress field. The situation is apparently more complex, however, since for most areas in the NEUS, the seismicity does not reveal any obvious alignments of epicenters along mapped faults or other known structural boundaries. It is thus quite difficult to prove the existence of any seismically active faults on a regional basis. Detailed studies of seismicity on a more local scale, especially results of aftershock monitoring of larger events, also yield ambiguous results with regard to the identification of active features. In this section, we discuss several examples of such detailed studies, and we conclude that an unequivocal correlation between mapped faults and earthquake activity is, at best, the exception rather than the rule.

Two relatively large earthquakes that occurred since the installation of the NEUSSN stations were the m_b 4.4 Gaza, NH earthquake of 1982 and the m_b 4.1 Dixfield, ME earthquake of 1983. In the case of these two earthquakes, as well as other relatively large earthquakes discussed in this section, m_b is given here rather than m_N because the events were large enough that m_b magnitudes were reported in the Regional Catalogue of Earthquakes (published by the International Seismological Centre). Both the Gaza, NH earthquake and the Dixfield, ME earthquake occurred in locations where field mapping has failed to show surface faults in the vicinity of the epicenters (Ebel and McCaffrey, 1984; Brown and Ebel, 1985).

Microearthquake swarms near Moodus, CT have occurred near a locality where a fault has been inferred but never confirmed (Ebel, 1985). Aftershocks of the m_b 3.8 earthquake near Bath, ME in 1979 occurred on or very near the Cape Elizabeth fault (Ebel, 1983). This may be evidence that, at least in some cases, earthquakes in the NEUS are associated with mapped faults. The mere spatial association of earthquakes with faults that are mapped near the surface, however, does not necessarily imply that the earthquakes are occurring on those faults. The faults could, for example, be the nucleation points for the earthquakes, yet the earthquake movements themselves may not have actually occurred on the preexisting fault surfaces. Furthermore, the larger earthquakes appear to be occurring at depths exceeding 5 km, and the orientation of faults mapped at the surface may be quite different from the orienation of faults at depth.

Another event of interest is the m_b 5.1 Goodnow, NY earthquake that occurred in the central Adirondack Mountains in 1983. That event was large enough to be felt throughout the NEUS and in southeastern Canada. Aftershock surveys provided a well constrained location for the source region. Seeber et al. (1984) argued that the aftershocks of the Goodnow earthquake occurred on a steeply-dipping fault striking N $15 \pm 10°$W beneath a NNW-striking surface lineament. The focal mechanism for this earthquake supports the trend seen in the aftershocks, but no surface fault breakage was found from the event. The aftershocks were confined to a depth range of 7 to 8.5 km, and there is no detailed information regarding the orientation of faults at that depth beneath the epicenter.

In the case of an earthquake near Lancaster, PA (m_{bLg} 4.1, April 23, 1984), the locations of the main event, aftershocks, and previous events in that region correlate well with mapped geologic lineaments. The mapped geologic lineaments also correlate with one fault plane of the focal mechanisms found for the 1984 events (Stockar and Alexander, 1986; Armbruster and Seeber, 1987). While such studies have indicated the possible orientations and positions of active faults, there are few, if any, cases in the NEUS where surface-mapped faults have been confirmed to be active.

EARTHQUAKE ACTIVITY IN THE NEW YORK CITY AREA

One of the proposed candidates for present-day seismic activity resulting from reactivation of ancient zones of weakness is found in the NYC area: the Ramapo Fault system in northern New Jersey and southeastern New York [Fig. 6(b)]. The Ramapo Fault system forms the northwestern margin of the Triassic-Jurassic Newark Basin. This fault system is about 120 km long, and it appears to have been active at various times throughout geologic history including the Precambrian, Paleozoic, Triassic, and Jurassic (Ratcliffe, 1971). Thus, the Ramapo Fault system could possibly be an example of a major throughgoing fault system that is being reactivated by the present-day stress field in the NEUS.

Aggarwal and Sykes (1978) concluded from analyzing locations, depths and focal mechanisms of earthquakes in the greater NYC area that seismic activity in that region is concentrated along several NE trending faults of which the Ramapo Fault appears to be the most active. More recent studies of earthquakes in the NYC area, however, suggest a more complicated relationship between earthquakes and geological features in this region. For example, Seborowski et al. (1982) argued that focal mechanisms of three earthquakes that occurred on or very near the Ramapo Fault have fault planes that are transverse to the mapped trace of the fault. Moreover, they argued that the microearthquake seismicity near the northern end of the Ramapo Fault trends NW, transverse to the trend of major geologic structures mapped at the surface. Also, Kafka et al. (1985) argued that earthquakes at least as large as those recorded near the Ramapo Fault have occurred as far as 50 km from that fault in a variety of geologic structures that surround the Newark Basin.

Based on the distribution of earthquakes recorded by the NEUSSN between 1975 and 1986, the Ramapo Fault does not appear to be any more active than numerous other locations in the NYC area [Fig. 6(b)]. There appear to be a number of locations in the NYC area that are at least as active as the area surrounding the Ramapo Fault. Indeed, the largest earthquake recorded by the NEUSSN stations in the NYC area occurred about 25 km from the mapped trace of the Ramapo Fault, near Ardsley, NY (October 19, 1985; m_b 3.6).

Fault plane solutions have been determined for the main shock, a foreshock and an aftershock of the Ardsley, NY earthquake (Filipkowski, 1986; Ebel and Kafka, 1989). These fault plane solutions suggest strike-slip faulting, with one possible fault plane trending NE (i.e. parallel to the trend of the Ramapo Fault) and the other plane trending NW (i.e. transverse to the Ramapo fault). Seeber and Dawers (1987) showed that there is a spatial correlation between a NW-striking mapped fault (the Dobbs Ferry Fault) and the earthquake activity near Ardsley, NY. The Ardsley earthquake

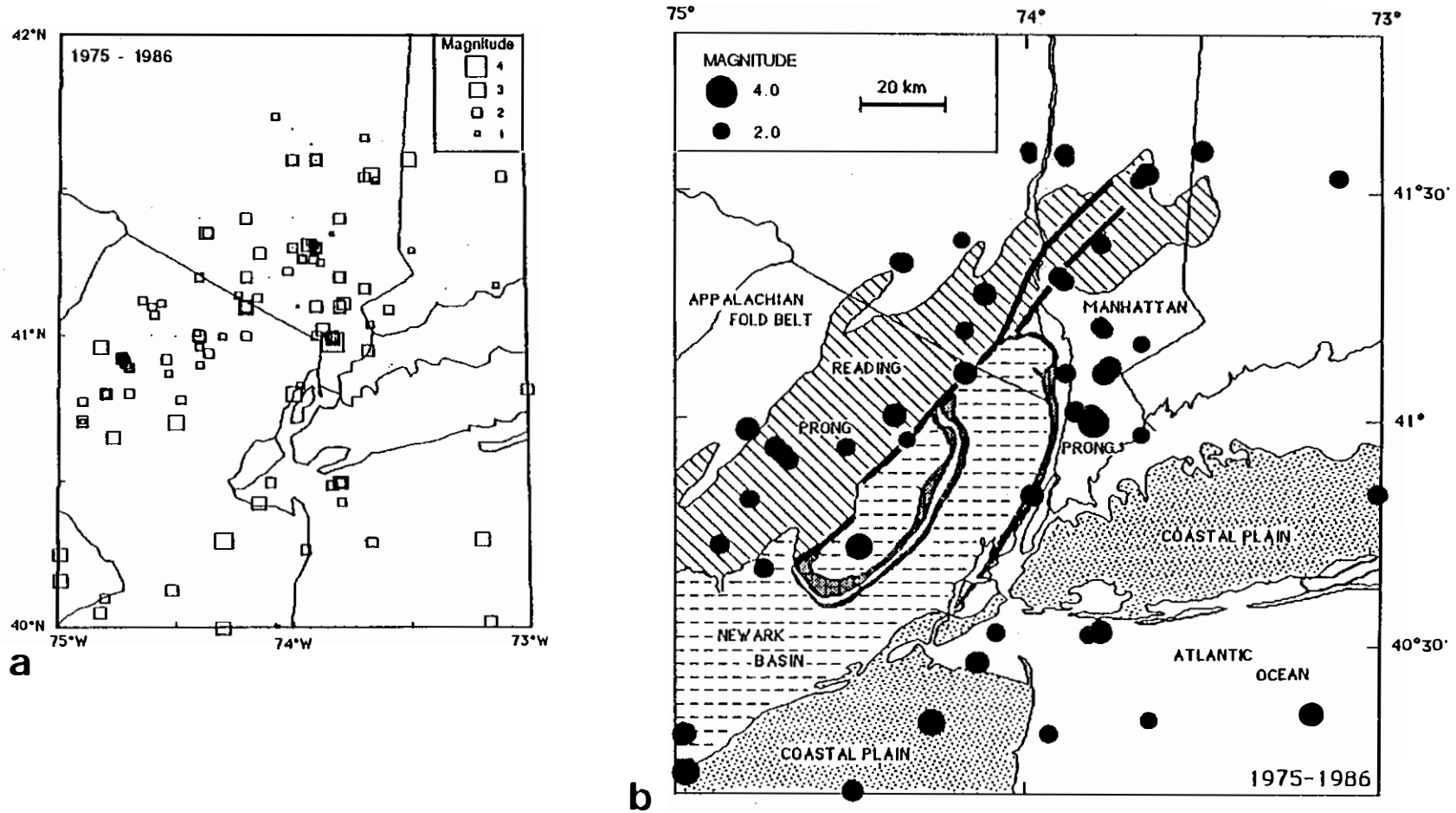

Figure 6. (a) Earthquakes recorded by stations of the NEUSSN in the greater NYC area. Magnitudes are m_N or m_C as published in the bulletins of the NEUSSN. (b) Earthquakes with m_N or $m_C \geq 2$ in the NYC area (1975-1986) and major geological features. Thick solid lines represent the surface trace of the Ramapo fault.

occurred at a depth of about 5 km, however, so that geological features mapped at the surface may be quite different from those that are in the vicinity of the hypocenter.

In the NYC area, it appears that the earthquake activity is broadly distributed throughout the geological features that surround the Newark Basin [Fig. 6(b)]. As in other parts of the NEUS, there are few, if any, cases in the NYC area where surface-mapped faults have been confirmed to be seismically active.

In this field trip we examine evidence for faulting (throughout geologic time) in the vicinity of the Ramapo Fault. As we have discussed above, the area surrounding the Ramapo Fault does not appear to be any more active than numerous other parts of the NYC area (Fig. 6). We have chosen this fault as a focus for this trip, however, not because it is has been confirmed to be seismically active, but rather because it is a prominent feature that exhibits many of the characteristics of geologic faults. This fault has been studied extensively, and it appears to have been active at various times throughout geologic history (Ratcliffe, 1971). In addition, this fault zone has been the focus of controversy related to issues of earthquake hazards at the Indian Point nuclear power plant (Aggarwal and Sykes, 1978), making it of some interest politically as well as scientifically.

GEOLOGY OF THE RAMAPO FAULT SYSTEM

The Ramapo Fault system marks the NE-trending boundary between the Newark Basin and the Hudson Highlands (Figs. 6b and 7). The Ramapo Fault proper extends from Peapack, NJ to the Hudson River near Stony Point, NY (Ratcliffe, 1971). The overall trend of the fault seems controlled by Grenville structures, i.e. by planes of weakness developed during late Precambrian. Outcrops along the Ramapo Fault west of the Hudson River place Precambrian metamorphic and igneous rocks of the Hudson Highlands against Triassic and Jurassic sedimentary rocks of the Newark Basin. Conglomerates near the border fault contain abundant clasts of Precambrian gneiss and Paleozoic cover rocks eroded from the uplifted Hudson Highlands (Carlson, 1946; Savage, 1968). Near Stony Point, outcrops of Paleozoic as well as Triassic rocks lie adjacent to the fault (Savage, 1968). Late Precambrian through Mesozoic displacements along the Ramapo Fault system include right-lateral, normal and reverse slip (Ratcliffe, 1981).

The Ramapo Fault can be followed as a clear, northeast-trending topographic lineament until north of Ladentown, NY (Fig. 7), where it splits into a N20°E-trending segment and one at N60°E connecting with the Thiells fault (Ratcliffe, 1980). The Mott Farm Road Fault extends northeastward and rejoins the main fault north of Tompkins Cove, NY (Ratcliffe, 1980). Alternatively, the main fault may be rotated westward and offset by the Willow Grove fault. If so, a NE-trending fault picks up again along Thiells Road. This second alternative would suggest that the Ramapo Fault is offset 4 km right-laterally. The age of this offset, however, is unknown.

Continuation of the Ramapo Fault across the Hudson River is problematic. It appears to follow either or both the Canopus Creek and Peekskill River valleys. In Peekskill Hollow, Paleozoic rocks lie next to Precambrian gneisses, marking the boundary of the Manhattan Prong. It is mainly a Paleozoic fault, although some Triassic and Jurassic reactivation may have occurred, each time resulting in the southeast side moving down (Ratcliffe, 1980). A complex, semi-ductile shear zone and a fracture zone extend along Canopus Creek, cutting across the structural grain of the Precambrian rocks. This fault zone locally places Paleozoic rocks next to Precambrian rocks (Ratcliffe, 1971). There is no direct evidence to support post-

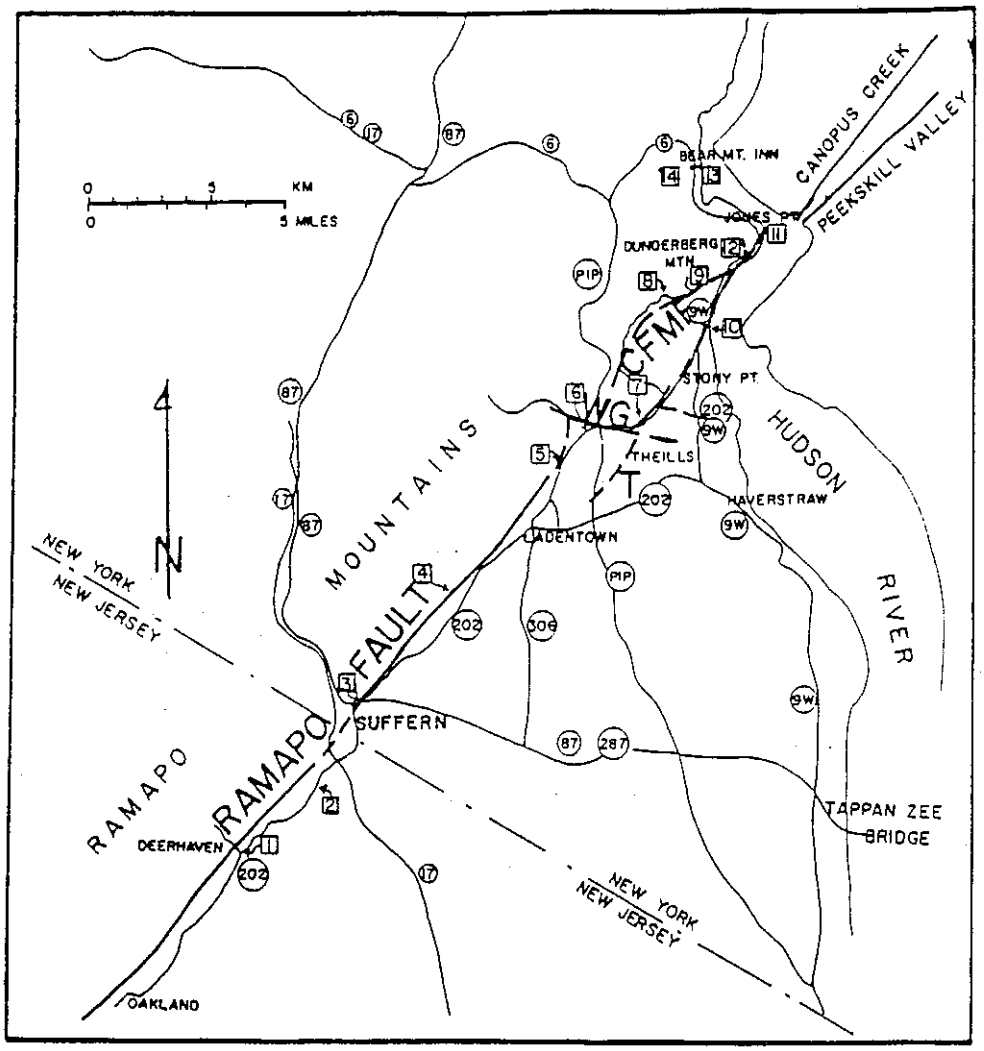

Figure 7. Road map and stops for field trip. Major faults shown as heavy lines may have Quaternary motion. WG = Willow Grove Fault; CFMF = Cedar Flats-Mott Farm Fault. T = Thiells Fault. Stop numbers in squares; Route numbers in circles.

Paleozoic motion east of the Hudson River along these faults (Ratcliffe, 1971; Ratcliffe, 1980). Structural and seismic evidence, however, support both valleys as possibly active faults (Seborowski et al., 1982).

Small-scale brittle structures within 100-200 m of the Ramapo Fault in several localities include conjugate oblique-normal faults (Ratcliffe, 1980). Both sets strike NE. Slickensides measured on the fault surfaces suggest that the SW-dipping set has right-oblique slip, while the NW-dipping set has predominantly left-oblique slip (Ratcliffe, 1980).

The dip of the fault, measured from drilling, is 45-70° SE, steepening toward the NE from Bernardsville, NJ to Stony Point, NY (Ratcliffe, 1980). Unhealed, unconsolidated rock gouge is found at each drilled locality. The fracture patterns, micro-offsets, and slickensides indicate that the northwest side has moved up. The dominant sense is right-oblique faulting. The maximum vertical offset is about 500 m (Ratcliffe, 1980).

GEOLOGIC EVIDENCE OF MOVEMENT ON THE RAMAPO FAULT SYSTEM DURING THE QUATERNARY

The Ramapo Fault stands out as a major structural feature in the NYC area. We examined evidence of Quaternary fault movements at some localities along the Ramapo Fault. The best geomorphic evidence of Quaternary fault movements consists of terrace development on one side of a valley, valley tilting, and systematic tributary offsets. These all indicate moderate slip of the Ramapo fault during the Quaternary.

To date, there is no clear evidence, however, of offset post-glacial material across faults in the NYC area (B. Stone, pers. comm., 1989). Pollen stratigraphy in wetlands along the Ramapo Fault near Ladentown, NY (Nelson, 1980) reveals no sudden changes in the post-glacial record. Unconsolidated cataclasites and gouge along the Ramapo Fault, however, may suggest post-Jurassic (Ratcliffe and Burton, 1984; 1985), or even younger, fault motion. Cores from glacial lake Passaic reveal slump folding, brecciation, and microfaulting (Forsythe and Chisholm, 1989). The features suggest antipodal reverse and normal components. Cumulative vertical displacements may be 1-2 meters.

ACKNOWLEDGEMENTS

This paper was reviewed by James Skehan, S.J., Randall Forsythe, and Dennis Weiss. We thank them for their helpful suggestions.

REFERENCES CITED

Aggarwal, Y. P., and Sykes, L. R., 1978, Earthquakes, faults, and nuclear power plants in southern New York and northern New Jersey: Science, v. 200, p. 4 25-529.

Armbruster, J.G. and L. Seeber, L., 1987, Seismicity and seismic zonation along the Appalachians and the Atlantic seaboard from intensity data: in K.H. Jacob (Editor), Proceedings of the Symposium on Seimic Hazards, Ground Motions, Soil-Liquefaction and Engineering Practice in Eastern North America, Technical Report NCEER-87-0025, 163-177.

Basham, P.W. and Kind, R., GRF broad-band array analysis of the 1982 Miramichi, New Brunswick earthquake sequence: Journal of Geophysical Research, v. 60, p. 120-128.

Bird, J. M., and Dewey, J. F., 1970, Lithosphere plate continental margin tectonics and the evolution of the Appalachian orogen: Geol. Soc. Am. Bull., v. 81, p. 1031-1060.

Brown, E. J., and Ebel, J. E., 1985, An investigation of the January 1982 Gaza, New Hampshire aftershock sequence: Earthquake Notes, v. 56, no. 4, p. 125-133.

Carlson, C.W., 1946, Appalachian drainage on the Highland border seidments of the Newark Series: Geol. Soc. Am. Bull., v.57, p. 997-1032.

Chaplin, M.P., Taylor, S.R., and Toksoz, M.N., 1980, A coda-length magnitude scale for New England: Earthquake Notes, v.51, p. 15-22.

Chase, C. G., 1979, Asthenospheric counterflow: a kinematic model: Geophys. Jour. Roy. Ast. Soc., v. 56, p. 1-18.

Ebel, J. E., 1983, A detailed study of the aftershocks of the 1979 earthquake near Bath, Maine: Earthquake Notes, v. 54, no. 4, p. 27-40.

Ebel, J. E., 1985, A study of Seismicity and Tectonics in New England: U. S. Nuclear Regulatory Commision Report, NUREG/CR-4354, 87 p.

Ebel, J. E., Vudler, V., and Celata, M., 1982, The 1981 microearthquake swarm near Moodus, Connecticut: Geophys. Res. Lett., v. 9, p. 397-400.

Ebel, J. E., and McCaffrey, S.J., J. P., 1984, The Mc=4.4 earthquake near Dixfield, Maine: Earthquake Notes, v. 55, no. 3, p. 21-24.

Ebel, J. E., Somerville, P. G., and McIver, J. D., 1986, A study of the source parameters of some large earthquakes of northeastern North America: Jour. Geophys. Res., v. 91, p. 8231-8247.

Ebel, J.E., and A.L. Kafka, A.L., 1989, Earthquake activity in the northeastern United States: in Decade of North American Geology, Volume GSMV-1, Neotectonics of North America, edited by D.B. Slemmons, E.R. Engdahl, D. Blackwell, D. Schwartz, and M. Zoback, in press.

Filipkowski, F., 1986, The use of short-period Rg waves as a depth discriminant for seismic events in the upper crust of the northeastern United States: [M.S. Thesis] Boston College, Chestnut Hill, MA, 81 p.

Forsythe, R. and L. Chisholm, 1989, Are there earthquake-induced deformation structures in the Highlands/Lowlands border region of New Jersey?, in Abstracts with Programs, 24th Annual Meeting of the Northeastern Geol. Soc. Am., v. 21, no. 2, p.15.

Graham, T., and Chiburis, E. F., 1980, Fault plane solutions and state of stress in New England: Earthquake Notes, v. 51, p. 3-12.

Hager, B. H., and O'Connell, R. J., 1979, Kinematic models of large-scale flow in the earth's mantle: Jour. Geophys. Res., v. 84, p. 1031-1048.

Herrmann, R. B., 1979, Surface wave focal mechanisms for eastern North American earthquakes with tectonic implications: Jour. Geophys. Res., v. 84(B7), p. 3543-3552.

Horner, R. B., Stevens, A. E., Hasegawa, H. S., and Leblanc, G., 1978, Focal parameters of the July 12, 1975 Maniwaki, Quebec earthquake--an example of intraplate seismicity in eastern Canada: Bull. Seism. Soc. Am., v. 68, p. 619-640.

Kafka, A.L., 1988, Earthquakes, geology and crustal features in southern New England: Seism. Res. Lett., v. 59, no. 4, p. 173-181.

Kafka, A.L. 1982, Seismicity and Geologic structures in the Manhattan prong: similarities and contrasts with the Hudson Highlands [abs.]: Earthquake Notes, vol. 53, no. 3, p. 20.

Kafka, A.L., E. Schlesinger-Miller, E. A. and N. L. Barstow, 1982, The Cheesequake, New Jersey earthquake of January 30, 1979: an inquiry into seismic activity in the Atlantic Coastal plain province of New Jersey [Abs.]: Earthquake Notes, v. 53, no. 3, p. 21.

Kafka, A.L., Schlesinger-Miller, E.A. and Barstow, N.L., 1985, Earthquake activity in the greater New York City area: Magnitudes, seismicity and geologic structures, Bull. Seism. Soc. Am., v. 75, 1285-1300.

Kirby, S. H., 1980. Tectonic stresses in the lithosphere: Constraints provided by the experimental deformation of rocks: Jour. Geophy. Res., v. 85, p. 6353-6363.

Linehan, S.J., D. and Leet, L.D., 1942, Earthquakes of the Northeastern United States and Eastern Canada, 1938, 1939, 1940: Bull. Seis. Soc. Am., v.32, p. 11-16.

Mrotek, K.A., Quittmeyer, R.C., Naumoff, P.G. and Statton, C.T., 1988, Observations of the earthquake swarm near Moodus, Connecticut: September/October 1987: [Abs.], EOS, Trans. Am. Geophys. Un., v. 69, no. 16, p. 495.

Nabalek, J. L., 1984, Determination of earthquake source parameters from inversion of body waves: [Ph.D. dissert.], Mass. Inst. of Technology, Cambridge, MA, 361 p.

Nelson, S., 1980, Determination of Holocene fault movement along the Ramapo fault in southeastern New York using pollen stratigraphy: in Abstracts with Programs, 15th Annual Meeting of the Northeastern Geol. Soc. Am., v. 12, no. 2, p.75.

Nuttli, O.W., 1973, Seismic wave attenuation and magnitude relations for eastern North America: Jour. Geophys. Res. v. 78, p. 876-885.

Pomeroy, P.W., Simpson, D.W., and Sbar, M.L., 1976, Earthquakes triggered by surface quarrying - the Wappingers Falls, New York sequence of June 1974: Bull. Seis. Soc. Am., v.66, p. 685-700.

Pulli, J. J., and Toksoz, M. N., 1981, Fault plane solutions for northeastern United States earthquakes: Bulletin of the Seismological Society of America, v. 71, p. 1875-1882.

Quittmeyer, R. C., Statton, C. T., Mrotek, K. A., and Houlday, M., 1985, Possible implications of recent microearthquakes in southern New York State: Earthquake Notes, v. 56, p. 35-42.

Ratcliffe, N. M., 1971, The Ramapo fault system in New York and adjacent northern New Jersey: a case of tectonic heredity: Geol. Soc. Am. Bull., v. 82, p. 125-142.

Ratcliffe, N. M., 1980, Brittle faults (Ramapo fault) and phyllonitic ductile shear zones in the basement rocks of the Ramapo seismic zone, New York and New Jersey, and their relationship to current seismicity: in Field Studies of New Jersey Geology and Guide to Field Trips, 52th Annual Meeting of the New York State Geol. Assoc Field Trip Guide, W. Manspeizer, ed., p. 278-312.

Ratcliffe, N. M., 1981, Reassessment of the Ramapo fault system as control for current seismicity in the Ramapo seismic zone and the New York recess: in Abstracts with Programs, 16th Annual Meeting of the Northeastern Geol. Soc. Am., v. 13, no. 3, p. 171.

Ratcliffe, N. M., and Burton, W.C., 1984, Brittle fault fabrics, mineralogy, and geometry of border faults of the Newark basin, NY-NJ from drillcore information: in Abstracts with Programs, 19th Annual Meeting of the Northeastern Geol. Soc. Am., v. 16, no. 1, p. 57.

Ratcliffe, N. M., and Burton, W.C., 1985, Fault reactivation models for origin of the Newark Basin and studies related to eastern U.S. seismicity: in Proceedings of the Second U.S. Geological Survey Workshop on the early Mesozoic basins of the eastern United States: U.S. Geological Survey Circular 946, G.P. Robinson and A.J. Froelich, eds., p. 36-46.

Richardson, R. M., Solomon, S. C., and Sleep, N. H., 1979, Tectonic stress in the plates: Rev. Geophys. and Space Phys., v. 17, p. 981-1019.

Rockwood, C.G. (1885). Notes on American earthquakes, No. 14, Am. J. Sci. (Ser 3), 29, 425-432.

Rosario, M. (1979). A coda duration magnitude scale for the New England seismic network, [M.S. thesis], Dept. of Geology and Geophysics, Boston College, Chestnut Hill, MA, 82 p.

Savage, E.L., 1968, The Triassic rocks of northern Newark Basin: in Guidebook to Field Excursions at the 40th Annual Meeting of the New York State Geological Association, R.M. Finks, ed., p. 49-68.

Sbar, M. L., Rynn, J. M. W., Gumper, F. J., Lahr, J. C., 1970, An earthquake sequence and focal Mechanism solution, Lake Hapatcong, northern New Jersey: Bull. Seism. Soc. Am., v. 60, p. 1231-1243.

Sbar, M. L., Armbruster, J., and Aggarwal, Y. P., 1972, The Adirondack, New York earthquake swarm of 1971 and tectonic implications: Bull. Seism. Soc. Am., v. 62, p. 1303-1317.

Sbar, M. L., Jordan, R. J., Stephens, C. D., Hickett, T. E., Woodruff, K. D., and Sammis, C. G., 1975, The Delaware-New Jersey earthquake of February 28, 1973: Bull. Seism. Soc. Am., v. 65, p. 85-92.

Schlesinger-Miller, E., Barstow, N. L., and Kafka, A. L., 1983, The July 1981 earthquake sequence near Cornwall, Ontario and Massena, New York: Earthquake Notes, v. 54, p. 11-26.

Seborowski, K. D., Williams, G., Kelleher, J. A., and Statton, C. T., 1982, Tectonic implications of recent earthquakes near Annsville, New York: Bull. Seism. Soc. Am., v. 72, p. 1601-1609.

Seeber, L., and Dawers, D., 1989, Characterization of an intraplate seismogenic fault in the Manhattan prong, Westchester Co., N.Y.: Seism. Res. Lett., v. 60, no. 2, 71-78.

Seeber, L. E., Cranswick, E., Armbruster, J., and Barstow, N., 1984, The Oct., 1983 Goodnow aftershock sequence, regional seismicity and structural features in the Adirondacks [Abs.], EOS, Trans. Am. Geophys. Un., v. 65, p. 240.

Skehan, S. J., J. W., 1988, Evolution of Iapetus Ocean and its borders in Pre-Arenig times: a synthesis: in The Caledonian-Appalachian Orogen: Geological Society Special Publication No. 38 (International Geological Correlation Program, Project 27), A. L. Harris and D.J. Fettes, eds., Blackwells Scientific Publications, Oxford, p. 171-215.

Skehan, S. J., J. W., and Rast, N., 1983, Relationship between Precambrian and Lower Paleozoic rocks of Southeastern New England and other North Atlantic Avalonian Terrains: in Regional Trends in the Geology of the Appalachian-Caledonian-Hercynian-Mauritanide Orogen, P.W. Schenk, ed., p. 131-162.

Smith, W. E. T., 1966, Earthquakes of eastern Canada and adjacent areas; 1928-1959: Pub. of the Dominion Observatory, Ottawa, Canada, v. 32, p. 87-121.

Stockar, D. V., and S. S. Alexander, 1986, The Lancaster seismic zone: Geologic and geophysical evidence for a north-south trending, presently active zone of weakness through Lancaster County, PA: [Abs.], EOS, Trans. Am. Geophys. Un., v. 67, p. 314.

Street, R., and Lacroix, A., 1979, An empirical study of New England seismicity: 1727-1977: Bull. Seism. Soc. Am., v. 69, p. 159-175.

Street, R. L., and Turcotte, F. T., 1977, A study of northeastern North American spectral moments, magnitudes and intensities: Bull. Seism. Soc. Am., v. 67, p. 599-614.

Sykes, L. R., 1978, Intraplate seismicity, reactivation of preexisting zones of weakness, alkaline magmatism, and other tectonism postdating continenta l fragmentation: Rev. Geophys. and Space Phys., v. 16, p. 621-688.

Wahlstrom, R., 1985, The North Gower, Ontario earthquake of 11 October, 1983: focal mechanism and aftershocks: Earthquake Notes, v. 56, no. 4, p. 35-143.

Weston Geophysical Research, Inc., 1977, The historical seismicity of New England, U.S. Nuclear Regulatory submittal docket No. SO-471 (DE S67601), 641 p.

Wetmiller, R. J., Adams, J., Anglin, F. M., Hasegawa, H. S., and Stevens, A. E., 1984, Aftershock sequences of the 1982, Mirmachi, New Brunswick earhquakes: Bulletin of the Seismological Society of America,, v. 74, p. 621-653.

Yang, J. P., and Y. P. Aggarwal, 1981, Seismotectonics on northeastern United States and adjacent Canada: Jour. Geophy. Res., v. 86, p. 4981-4998.

RAMAPO FAULT FIELD TRIP

In this field trip, we will examine geologic features that might be related to earthquakes, and we will look for characteristics that might identify active and non-active faults. Of several geomorphological features possibly associated with Quaternary age faulting in the NEUS, a few well-defined examples stand out in the NYC area (Figs. 6b and 7). These features appear to concentrate along the Ramapo Fault zone and the Hudson River valley. This field trip will visit several localities along the distinctive topographic lineament of the Ramapo fault system where geomorphic features suggest Quaternary displacements. These features include the following:

(1) Fault scarps (primary and secondary) along the length of the Ramapo Fault system.
(2) Different heights, numbers, and ages of river terraces across the Ramapo and Mahwah Rivers.
(3) Asymmetric valleys with river running against the faulted side of the valley. This suggests continued tilting of fault blocks (e.g. Ramapo and Mahwah Rivers).
(4) Narrow zones of unconsolidated fault gouge in soil along the Ramapo Fault.
(5) Repeated offset tributaries to the Ramapo river suggesting dextral shear.
(6) Migrated meander loops of the Ramapo River suggesting dextral shear.

Some features, such as offset tributaries, valleys, and asymmetric meanders are better observed on maps and aerial photos than on a field trip. Other tectonically-controlled landforms, such as reversal of river drainage direction, changes in tilt of the Palisades sill, offsets in the sill, and abrupt changes in height of its basal contact, post-date the early Mesozoic, but cannot be proven to be Quaternary in age.

The field trip follows the trace of the Ramapo fault along the Ramapo River in NJ and the Mahwah River in NY. South of Suffern, the Ramapo fault system forms a well-defined linear feature. At Suffern, however, it appears to split into two or more splays beneath a floodplain. The lineament following the Mahwah River marks the boundary between the Hudson Highlands and the Newark Basin. The field trip will follow the Mahwah River to its headwaters, where the Ramapo fault appears to split or be truncated by the Willow Grove Fault. North of Willow Grove, a NE-trending fault can be followed to the Hudson River.

The presence of greater numbers and heights of river terraces on the west side of the Ramapo and Mahwah River valleys along the boundary between the Hudson Highlands and Newark Basin support uplift of the NW side of the valley, the Hudson Highlands, along the Ramapo fault. The regular spacing of the terraces down to the present river edge suggests episodic uplift during the Quaternary. The absence of terraces on the SE side of the river valleys appears to be independent of lithology. In other words, the river terraces on the NW side appear to be tectonic.

Several right-slip offsets of cross-strike (SE-flowing) tributaries occur where they empty into the Ramapo River. Two meanders of the Ramapo also appear to be structurally controlled. They also support Quaternary age right-slip motion.

ROAD LOG FOR FIELD TRIP: EARTHQUAKE ACTIVITY IN THE GREATER NEW YORK CITY AREA

To begin this field trip: from the North, take Routes 6 and 17 east to the NY State Thruway I-87 (Exit 16). Take the Thruway south 16 miles to Exit 15 (Route 17 South to NJ). From the South, follow the Thruway north (I-87 and I-287) from the Tappan Zee Bridge or intersect the Thruway northbound from Exit 9 of the Palisades Interstate Parkway. Take Exit 15 of the Thruway, the second Suffern exit. Follow signs to Route 17 south toward NJ. Mileage begins once exit ramp merges with Route 17 South.

CUMULATIVE MILEAGE	MILES FROM LAST POINT	ROUTE DESCRIPTION
0.0	0.0	Route 17 southbound lane.
1.0	1.0	Exit to Route 202 on right. At the stop sign turn left onto Route 202 South. The Ramapo fault lies to the west between the Ramapo Mountains and the Ramapo River.
3.0	2.0	Pass Ramapo Reservation sign on right.
4.6	1.6	Turn right at small bridge with historical sign and horse crossing marker. Cross the Ramapo River.

STOP 1. DEERHAVEN.

The topography rises toward the west in discrete steps forming several discontinuous terraces on the NW side of the Ramapo River valley. They are not matched on the SE side. The terraces have formed on both unconsolidated sediment and bedrock. Notice how the river flows to the NW side of the valley along most of its length, regardless of the topographic and bedrock changes on the SE side of the river. This suggests westward tilting of the valley toward the fault. Bear Swamp Brook cuts perpendicular to the structure (SE). Upstream its banks are inequal in height. The NE side appears to be higher, as is the case for several other cross-strike streams that cross the Ramapo fault trace.

4.7	0.1	Turn left and cross small creek. The houses are built on a higher level. Follow the road south then west up to a higher level. Take a left at Deerhaven Road which follows a higher level.
5.2	0.5	At T-intersection make a right to go up hill. At fork make right and go up hill to discontinuous outcrops of crystalline rocks.
5.5	0.3	End of road. Return by same route. Notice the asymmetry of the cross-sectional view of the Ramapo River valley.
6.4	0.9	Return to Route 202 and proceed north.
8.0	1.6	Turn left at Ramapo Reservation sign, park at the south end of the parking lot.

STOP 2. RAMAPO RESERVATION.

This stop involves a 30 minute round-trip hike. Follow a trail directly west to a bridge over the Ramapo River. Cross abandoned meander loops and marshy areas. Across the river is a large lake in a wide, flat flood plain. Begin to climb upward. Return to parking area. Exit to south only.

8.2	0.2	Proceed north on Route 202.
9.0	0.8	Pass entrance to Ramapo College on right.
10.3	1.3	Pass under Route 17. Stay on Route 202.
11.3	1.0	Pass under railroad bridge to stop. LOW CLEARANCE! Turn left to remain on Route 202.
12.0	0.7	Take a sharp left immediately after Thruway overpass onto Pavilion Road. Proceed uphill and park halfway up the hill in the Knights of Columbus parking area.

STOP 3. PAVILION ROAD.

Near the bottom of the hill are exposures of slickensided crystalline rock, one of the few outcrops of the Ramapo fault. These well-developed slickensides of unknown age suggest dip-slip movement with a minor right-slip component. Slickensided fault surface averages N 55-65°E, and dips 60-65°SE. Slickenlines pitch N 15°E, 55°SE.

12.7	0.2	Return to the intersection with Route 202 and proceed north. Route 202 runs along one terrace level above the Mahwah River that is not present on the eastern side. Some discontinuous, higher terrace levels can be seen on the west side of the road.
16.3	3.6	Turn left onto Sky Meadow Road.

STOP 4. SKY MEADOW ROAD.

Proceed southwest and west down across the Mahwah River, driving toward the fault. The road climbs four well-developed levels between the river and the fault. Power lines on the mountain follow a natural bench for several kilometers. The river valley is terraced on the NW side, and is hummocky and irregular on the SE side. Drilling data near here suggest that a Triassic age vesicular lava flow, over 450 ft thick, accumulated near the border fault (Ratcliffe, 1980). Local relief at the edge of the basin at the time was approximately 450 feet (Ratcliffe, 1980).

16.6	0.3	Intersection. Turn around. Return to Route 202.
16.9	0.3	Intersection of Sky Meadow Road and Route 202. Turn left onto Route 202.
19.4	2.5	At traffic light turn left. Maps say Ladentown.
19.5	0.1	Turn right at intersection onto Old Route 306.
19.8	0.3	Turn left at sign for Call Hollow Road. This road runs parallel to the Ramapo fault. The river valley narrows toward the north. The

		fault lies on the west side of the river valley. The topography rises on both sides of the road. However, on the east side, the landforms are hummocky and irregular, whereas on the west side of the river, there are distinct levels. The power lines follow one wide terrace.
21.5	0.7	Park on the right side where the power lines cross the road.

STOP 5. CALL HOLLOW ROAD.

North of Ladentown and just south of Willow Grove on Call Hollow Road the ridge defining the eastern edge of the Hudson Highlands begins to turn north as you approach the Willow Grove Valley. The Mahwah River valley pinches out. The terrace along which the power lines have run also ends here. The lines cross the road to join a buried gas line that follows the NW-trending steep ridges and narrow valley. These features also truncate in Willow Grove valley. The gas line is buried in intensely fractured material. Triassic basalts on the W side of the road tilt SE.

21.5	0.0	Proceed north on Call Hollow Road. The Ramapo fault no longer forms a clear topographic lineament toward the north.
22.4	0.9	Park directly under the power lines.

STOP 6. WILLOW GROVE.

The Ramapo fault cannot be easily followed north of Willow Grove valley. The fault appears to trend more toward the north and to be offset about 4 km right laterally by an E-SE-trending fault that follows Minisceongo Creek through Willow Grove valley. The creek experiences several 90° bends near Willow Grove. The terrain to the north and west of Willow Grove consists of massive, rounded hills with short, non-linear valleys as is typical of the topography west of the Ramapo fault. An alternative suggestion is that Willow Grove valley could be a pull-apart developed between the diverging splays of the Ramapo and Theills faults. The saddle to the south consists of highly brecciated rock fragments.

22.6	0.6	At the stop sign at the bottom of the hill, turn right onto Willow Grove Road. Proceed east along Minisceongo Creek.
23.1	0.5	Pass under Palisades Parkway.
24.2	1.1	At Hammond Road (unmarked), bear left.
24.4	0.2	Turn left onto Theills Road; park on the right.

STOP 7. THEILLS ROAD.

Here the best candidate for a continuation of the Ramapo fault is seen to follow the NE-trending section of Cedar Pond Brook. Terraces are seen only on the NW side of the stream valley. Once again it represents hilly Hudson Highlands juxtaposed next to Quaternary sediments. Notice here, too, that there are river terraces only on the NW side of the valley, and that the SE side is lower. Between Call Hollow Road and Theills Road is a possible horst block of Proterozoic gneiss (Ratcliffe, 1980). NE-striking features in the area do not seem to offset lava flows, but discontinuous

exposures do not allow confirmation of any post-Mesozoic movements, except for tilting of basaltic layers.

25.2	0.8	Turn left (west) onto Cedar Pond Road (Route 210)
26.5	1.3	Turn right onto Cedar Flats Road. Old schoolhouse on the right. Cedar Flats Road and Mott Farm Road parallel the fault.
28.2	1.7	Past Queensboro Road turn left toward the sign for "Camp Addisone-Boyce". This is Mott Farm Road (unmarked). The road detours around Lake Bullowc. The fault continues on NW side of the lake. The road then resumes its trend parallel to the possible fault.
29.2	1.0	Pass sign for Camp Addisone-Boyce.
29.5	0.3	Park on right after 20 ft high outcrop on left.

STOP 8. MOTT FARM ROAD.

Slickensided surfaces, vertical to steeply dipping. Some slickensided surfaces dip steeply SW with slickenlines plunging 65-75°SW. Other surfaces dip steeply NW with slickenlines plunging 75-80°NE. Several fracture patterns are also evident.

29.8	0.3	Pass outcrop of brecciated rock with complex fracture patterns.
30.1	0.3	Birdhill Road. Left on Fairview.
30.5	0.4	At Tompkins Lake, follow road around toward north on natural terrace 2-3 meters high which is not present on the other side. Steep talus slope rises to west.
30.8	0.3	Stop 9.

STOP 9. TOMPKINS LAKE.

View of terrace and former lake level. Return to main road via Birdhill Road.

31.7	0.9	Birdhill Road intersection with Mott Farm Road. Turn left (east).
32.4	0.7	Pass intersection with Gays Hill Road.
32.65	0.25	Mott Farm Road and Route 9W intersection. Turn right and proceed south.
33.25	0.6	Turn left onto Elm Street. It is a sharp turn. Take the first left. Follow the road down the hill. At the power station, turn right.
33.8	0.55	Park at the large limestone outcrop at the entrance to the Tompkins Cove quarry next to the Lovett power plant.

STOP 10. TOMPKINS COVE QUARRY.

Cambro-Ordovician limestone beds with black chert interbeds and bedding-parallel stylolites trend N 10-20°E and dip 55-65°SE. Calcite-filled fractures cut the outcrop at N 20-30°E and dip 40-42°SW. The brittle features could be related to the Ramapo fault

system. See Ratcliffe (1980) for further information. The quarry reveals eight fault zones that disrupt the structural continuity (Ratcliffe, 1980). The faults are identifiable as red or green zones of clay gouge and phyllonite, best seen on the south face of the quarry on all levels. These faults are SE-dipping reverse faults with left- or right-lateral offsets. Despite a youthful appearance, they are associated with folds (Ratcliffe, 1980) although they appear to have been reactivated to produce the clay gouge and slickensides. Ratcliffe suggests that the faults are pre-Mesozoic thrusts that were reactivated during the Triassic as normal and strike-slip faults.

34.2	0.4	At intersection of Elm Street and Route 9W, turn right (north).
34.8	0.6	Pass intersection with Mott Farm Road.
35.8	1.0	Intersection of Gays Hill Road and Route 9W. Turn right (north) onto Route 9W. Slickensided surfaces on a new outcrop exposed on left at mile point 36.0. No stop here. As you proceed north on Route 9W, the Ramapo fault or Mott Farm Road fault runs close to the river. Route 9W is adjacent to or on the fault. Recent construction on Route 9W has revealed rich zones of slickensides, intensely fractured rock, and brecciated zones along this stretch of road.
36.8	1.0	Bear right leaving Route 9W for Jones Point Road. The road follows along a river terrace. There is also a lower level, and the remnant of a higher one. Turn right at the "T", then left to continue north along the lower terrace. These terraces are not present on the east side of the Hudson River valley in this vicinity.
37.5	0.7	Park along the railroad right-of-way at the end of the road.

STOP 11. JONES POINT.

Jones Point is built on a series of low terraces. Walk along the railroad bed toward the north. STAY OFF THE TRACKS! The fault also outcrops immediately behind the house. At the intersection of the road and the railroad tracks is a polished and grooved outcrop that marks the end of the crystalline rocks in this area. The steep, SE-facing fault surface is polished and has sub-horizontal glacial grooves. Small normal faults are seem on the exposure. Note that where the fault crosses the Hudson River, the river abruptly changes direction. The Indian Point power plant is located directly across the Hudson River to the east. The Canopus and Peekskill River valleys are visible from here.

37.8	0.3	Return by the same route, take right fork to view a possible older terrace and till remnant near a former chapel.

38..1 0.3 Cross Route 9W and pull immediately into a wide pull-over and park.

STOP 12. ABANDONDED QUARRY.

The Ramapo fault cuts the south side of the hill. Between this site and the river are several low terraces. Note truncated (over-steepened) spurs here. Walking west over a wide flat area, there is a possible scarp and sag pond in the area not exploited by the former quarry. The small scarp is 1-1.5 meters high. The terrace is developed on stream cobbles of a former river level.

38.1	0.0	Proceed north on Route 9W.
40.8	2.7	Take left fork in road for Bear Mountain State Park and Inn (Route 6).
41.5	0.7	At traffic circle, take first right for Bear Mountain Inn.
41.9	0.4	Turn left into parking lot.

STOP 13. BEAR MOUNTAIN INN.

Refreshments, etc. The only scheduled rest stop.

42.0	0.1	Leave Bear Mountain Inn. Turn right onto Route 6. At 42.3 mile point, Bear Mt. Circle, take first right; continue on Route 6 west.
44.0	2.1	Turn right at sign to Perkins Memorial Drive. Proceed to top of mountain to lookout. No mileage.

STOP 14. PERKINS MEMORIAL DRIVE LOOKOUT.

The Ramapo fault crosses the Hudson River to enter the Peekskill Hollow or Canopus River valleys. Sharp bends in the Hudson River appear to be structurally controlled. Each linear river bend, when projected onshore in Westchester or Rockland County, is associated with an anomalously linear river valley that follows the same strike. Some examples include the Ramapo, Mahwah, Cedar Pond, Minisceongo, Canopus, Leeds Cove, and Peekskill Hollow valleys. The terrace on the NW side of the Peekskill river appears to be higher than on the east side.

On a regional scale, the Hudson River is linear and trends N-S, except where crystalline rocks cross it. At least one of the NE-trending segments occurs where the Ramapo fault crosses the Hudson. Another SE jog occurs where the Willow Grove fault crosses the river. The trend of another sharp bend in the Hudson River toward the SE follows a lineament onshore into Westchester County along the linear Leeds Cove valley. This latter example suggests that the Ramapo fault offsets one kilometer right-laterally a possible fault beneath the Hudson River.

Turn right onto Route 6 and proceed west. After a forced merge with the Palisades Interstate Parkway either proceed south toward New York City or take Exit 18 to remain on Route 6 West. At traffic circle, take first right onto Route 6 West and continue to Routes 6, 17, or the New York Thruway.

NOTES